

Report Number 11/73

**Filling of a Poisson trap by a population of random intermittent
searchers**

by

Paul C. Bressloff and Jay M. Newby



Oxford Centre for Collaborative Applied Mathematics
Mathematical Institute
24 - 29 St Giles'
Oxford
OX1 3LB
England

Filling of a Poisson trap by a population of random intermittent searchers

Paul C. Bressloff^{1,2} and Jay M. Newby²

¹*Department of Mathematics, University of Utah, 155 South 1400 East, Salt Lake City UT 84112*

²*Mathematical Institute, University of Oxford, 24-29 St. Giles', Oxford, OX1 3LB, UK*

We extend the continuum theory of random intermittent search processes to the case of N independent searchers looking to deliver cargo to a single hidden target located somewhere on a semi-infinite track. Each searcher randomly switches between a stationary state and either a leftward or rightward constant velocity state. We assume that all of the particles start at one end of the track and realize sample trajectories independently generated from the same underlying stochastic process. The hidden target is treated as a partially absorbing trap in which a particle can only detect the target and deliver its cargo if it is stationary and within range of the target; the particle is removed from the system after delivering its cargo. As a further generalization of previous models, we assume that up to n successive particles can find the target and deliver its cargo. Assuming that the rate of target detection scales as $1/N$, we show that there exists a well-defined mean field limit $N \rightarrow \infty$, in which the stochastic model reduces to a deterministic system of linear reaction-hyperbolic equations for the concentrations of particles in each of the internal states. These equations decouple from the stochastic process associated with filling the target with cargo. The latter can be modeled as a Poisson process in which the time-dependent rate of filling $\lambda(t)$ depends on the concentration of stationary particles within the target domain. Hence, we refer to the target as a Poisson trap. We analyze the efficiency of filling the Poisson trap with n particles in terms of the waiting time density $f_n(t)$. The latter is determined by the integrated Poisson rate $\mu(t) = \int_0^t \lambda(s)ds$, which in turn depends on the solution to the reaction-hyperbolic equations. We obtain an approximate solution for the particle concentrations by reducing the system of reaction-hyperbolic equations to a scalar advection-diffusion equation using a quasi-steady-state analysis. We compare our analytical results for the mean-field model with Monte-Carlo simulations for finite N . We thus determine how the MFPT for filling the target depends on N and n .

PACS numbers: 05.40.-a, 87.10.-e

I. INTRODUCTION

There are many examples in nature where random search strategies provide an efficient means for locating one or more targets of unknown location. Examples include animals foraging for food or shelter, [1–4], the active transport of reactive chemicals in cells [5–9], a promoter protein searching for a specific target site on DNA [10–13], and the motor-driven transport and delivery of vesicles to synaptic targets along the axons and dendrites of neurons [14–17]. One particular class of model that has been applied both to foraging animals and active transport in cells, treats a random searcher as a particle that switches between a slow motion (diffusive) or stationary phase in which target detection can occur and a fast motion ‘ballistic’ phase; transitions between bulk movement states and searching states are governed by a Markov process [18–21]. If the random search is unbiased and the probability of finding a single hidden target is unity, then it can be shown that there exists an optimal search strategy given by the durations of each phase that minimize the mean first passage time (MFPT) to find the target. Motivated by experimental observations of the motor-driven transport of mRNA granules in dendrites [22, 23], we have recently extended a one-dimensional (1D) version of these models to the case of a directed intermittent search process, in which the motion is directionally biased and there is a non-zero probability of failing to find the target (due to competition with other targets or degra-

dation) [16, 17]. In this case there no longer exists an optimal search strategy, unless additional constraints are imposed such as fixing the target hitting probability.

In this paper, we extend the continuum theory of random intermittent search processes to the case of N independent searchers looking to deliver cargo to a single hidden target located somewhere on a semi-infinite track. We assume that all of the particles start at one end of the track and realize sample trajectories independently generated from the same underlying stochastic process. For simplicity, we consider a 3-state Markov process in which each particle can be in one of three internal states: stationary, moving to the right (anterograde) with speed v , or moving to the left (retrograde) with speed $-v$. The hidden target is treated as a partially absorbing trap in which a particle can only detect the target and deliver its cargo if it is stationary and within range of the target; the particle is removed from the system after delivering its cargo. As a further generalization of previous models, we assume that up to n successive particles can deliver their cargo to the target. Assuming that the rate of target detection scales as $1/N$, we show that there exists a well-defined mean field limit $N \rightarrow \infty$, in which the stochastic model reduces to a deterministic system of linear reaction-hyperbolic equations for the concentrations of particles in each of the internal states. In the mean-field limit, these equations decouple from the stochastic process associated with filling the target with cargo. The latter can be modeled as a Poisson process in which the

time-dependent rate of filling the target $\lambda(t)$ depends on the concentration of stationary particles within the target domain. We thus refer to the target as a Poisson trap.

We analyze the efficiency of filling the Poisson trap with n particles in terms of the waiting time density $f_n(t)$. In the case of a semi-infinite track, the probability of successfully filling the target is equal to unity when the search is unbiased, that is, the so-called hitting probability $\Pi_n \equiv \int_0^\infty f_n(t)dt = 1$. On the other hand, $\Pi_n < 1$ for a biased search. The waiting time density is determined by the integrated Poisson rate $\mu(t) = \int_0^t \lambda(s)ds$, which in turn depends on the solution to the reaction-hyperbolic equations for the concentrations. We obtain an approximate solution to these equations by carrying out a quasi-steady-state (QSS) reduction along analogous lines to our previous work on molecular-motor-based models of single searchers [17, 24]. This generates a scalar advection-diffusion equation for the concentrations. The QSS reduction is applicable provided the Markov transition rates between internal states of a particle are fast compared to the velocities on an appropriately defined spatial scale. We also compare our analytical results for the mean-field model with Monte-Carlo simulations for finite N . A number of results follow from our study. First, the mean-field model exhibits the same qualitative behavior as found in previous single searcher models, namely, there exists an optimal search strategy in the case of unbiased search but not in the case of directed intermittent search. Second, we quantify how increasing the number of searchers N reduces the MFPT for filling the target and increases the hitting probability (in the case of biased search). Third, we quantify how the hitting probability decreases and the MFPT increases as we increase the capacity n of the target or trap.

It should be noted that there have been some previous studies of multiple searchers looking for a single target, but in discrete space on a 1D infinite lattice [25, 26]. At each time step, a searcher jumps to a neighboring site with probability α in either direction, which is a discrete version of the diffusive phase in continuum models. With probability $(1-\alpha)$ the particle leaves the lattice for a fixed duration T , after which it lands at some distance L from its initial position in either direction. This phase corresponds to the ballistic non-search phase. The duration of the diffusive phase with target detection is exponentially distributed with mean duration $1/(1-\alpha)$. Oshanin *et. al.* [25, 26] have shown that in the thermodynamic limit $N \rightarrow \infty$ (with the mean density of searchers fixed), the probability, that at a given time t , the target has been found by any one of the searchers has a maximum at an optimal value of α (which depends on t). A related discrete model has been considered by Rojo *et. al.* [27]. In addition to being lattice models rather than continuum models, these previous studies also focus on unbiased searches in which the target is a perfect absorber.

The basic structure of the paper is as follows. In section II we develop the mean-field population model, and

determine the form of the waiting time density for filling the Poisson trap. The time-dependent rate $\mu(t)$ is calculated in section III by carrying out a QSS reduction of the mean-field model. We also determine the asymptotic behavior of the waiting time density. Our numerical results are presented in section IV, and a Gaussian approximation of the waiting time density for a large capacity trap is derived in the Appendix.

II. MEAN-FIELD POPULATION MODEL

Consider a population of particles moving along a semi-infinite track, $0 \leq x < \infty$. Such a track could represent a system of oriented microtubular filaments within the dendrite or axon of a neuron, with each particle corresponding to a motor-driven cargo complex, see Fig. 1 and [14, 16]. (Real axons and dendrites are of finite extent; we will assume that boundary effects at the far end of these structures can be neglected by considering a semi-infinite track. For simplicity, we also neglect the effects of branching, although this can also be taken into account [17]). All particles are injected on to the track at the end ($x = 0$). This would correspond to motor-driven particles entering a primary dendrite from the soma of a neuron, for example. Particle injection can either be treated as an initial condition, representing the sudden introduction of a large bolus of particles at $x = 0$, or treated as a boundary condition in which there is a fixed particle flux at $x = 0$. We will focus on the former case here. Within the interior of the track each particle is taken to be in one of three states labeled by $n = 0, \pm$: stationary ($n = 0$), moving to the right (anterograde) with speed v ($n = +$), or moving to the left (retrograde) with speed $-v$ ($n = -$). Assuming that transitions from the moving states $\pm v$ to the stationary state occur at the fixed rates β_\pm and the reverse transitions occur at the rate α , we can write down the following system of equations for the concentrations $u_n(x, t)$ of particles in state n at time t and position x along the track:

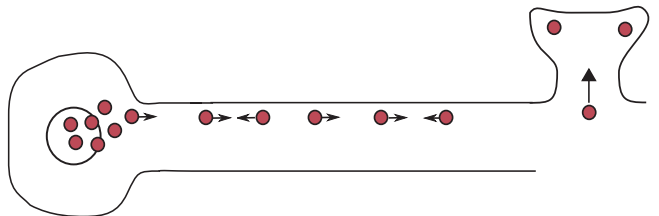


FIG. 1. Schematic diagram illustrating a population model of motor-driven particles moving along a one-dimensional track. The particles can transition from a moving state with velocity $\pm v$ at a rate β_\pm and from a stationary searching state at a rate α . A partially absorbing trap is located at $x = X$ that fills up according to a Poisson process.

$$\partial_t u_+ = -v\partial_x u_+ - \beta_+ u_+ + \alpha u_0 \quad (2.1a)$$

$$\partial_t u_- = v\partial_x u_- - \beta_- u_- + \alpha u_0 \quad (2.1b)$$

$$\partial_t u_0 = \beta_+ u_+ + \beta_- u_- - 2\alpha u_0. \quad (2.1c)$$

Equation (2.1) is supplemented by a zero flux boundary condition at $x = 0$:

$$v[u_+(0, t) - u_-(0, t)] = 0. \quad (2.2)$$

In the case of an initial bolus of size U , the corresponding initial condition is $u_n(x, 0) = U\delta_{n,+}\delta(x)$. We also assume that the bidirectional transport process is biased in the anterograde direction by taking $\beta_+ \leq \beta_-$; the limit $\beta_- \rightarrow \infty$ corresponds to unidirectional transport.

The system (2.1) belongs to a general class of linear reaction–hyperbolic equations studied previously by a number of groups [14, 28–30]. Under the assumption that the transition rates are sufficiently fast, Reed *et al.* [14] used singular perturbation methods to carry out an asymptotic expansion of a solution whose leading order term is given by an approximate traveling wave solution of a corresponding one–dimensional advection–diffusion equation. They then showed how such a solution matches wave–like behavior observed experimentally in the fast axonal transport of vesicles. The validity of this reduction was subsequently proved rigorously under a wide range of conditions [28, 29]. Probabilistic versions of these axonal transport models have also been developed [30, 31].

In this paper we consider the following problem: given the temporal profile of particle concentrations, how quickly can a target at some location X on the track fill up with cargo? The target could correspond to a synapse or an intracellular pool within an axon or dendrite. We will assume that a particle can only deliver its cargo if it is within a distance l of the target and is in the stationary state. Delivery of cargo to the target is then modeled as an inhomogeneous Poisson process with time–dependent rate

$$\lambda(t) = \kappa \int_{X-l}^{X+l} u_0(x, t) dx. \quad (2.3)$$

That is, the rate depends on the average concentration of stationary particles within the target domain, and we refer to the target as a Poisson trap. Let the discrete stochastic variable $M(t)$ denote the number of particles that have delivered their cargo at time t given that $M(0) = 0$. It follows that

$$P(n, t) \equiv \Pr[M(t) = n] = \frac{\mu(t)^n e^{-\mu(t)}}{n!}, \quad (2.4)$$

where

$$\mu(t) = \int_0^t \lambda(s) ds. \quad (2.5)$$

We are interested in how long it takes to deliver n cargoes to the target. This is given by the waiting time W_n , which

is the time of the n^{th} event (delivery of the n^{th} cargo). In particular, we want to determine the waiting time density $f_n(t)$ with $f_n(t)dt = \Pr[t \leq W_n < t + dt]$, from which we can calculate the filling probability Π_n and conditional mean first passage time (MFPT) T_n for n to be reached, where

$$\Pi_n = \int_0^\infty f_n(t) dt, \quad T_n = \frac{\int_0^\infty t f_n(t) dt}{\int_0^\infty f_n(t) dt}. \quad (2.6)$$

Note that in reality a trap will have a finite capacity M so that $n \leq M$. This modifies the expression (2.4) in the case $n = M$, that is,

$$P(M, t) = 1 - \sum_{n=0}^{M-1} \frac{\mu(t)^n e^{-\mu(t)}}{n!}. \quad (2.7)$$

However, we don't have to worry about this boundary effect in our subsequent analysis, since we will focus on first passage time processes. Also note that in the large M limit, we can carry out a Gaussian approximation of the Poisson process for filling the trap, see the appendix.

Waiting time density

The density $f_n(t)$ can be expressed in terms of the integrated rate $\mu(t)$ as follows [32]. Let $F_n(t) = \Pr[W_n \leq t]$ be the cumulative waiting time distribution such that $f_n(t) = dF_n(t)/dt$. Since by definition $\Pr[W_n \leq t] = \Pr[N(t) \geq n]$, it follows that

$$\begin{aligned} F_n(t) &= \sum_{k=n}^{\infty} \frac{\mu(t)^k e^{-\mu(t)}}{k!} \\ &= 1 - \sum_{k=0}^{n-1} \frac{\mu(t)^k e^{-\mu(t)}}{k!}. \end{aligned} \quad (2.8)$$

Differentiating both sides with respect to t , we find that all terms cancel except for one, leading to the result

$$f_n(t) = \frac{\mu'(t)\mu(t)^{n-1}e^{-\mu(t)}}{(n-1)!}. \quad (2.9)$$

In the case of a constant rate $\lambda(t) = \lambda$, $f_n(t)$ is given by a gamma distribution:

$$f_n(t) = \lambda \frac{(\lambda t)^{n-1} e^{-\lambda t}}{(n-1)!} \quad (2.10)$$

so that $\int_0^\infty f_n(t) dt = 1$. It follows that the filling probability $\Pi_M = 1$, that is, the trap will be filled to capacity with unit probability. On the other hand, in the case of a time–dependent rate, the filling probability may be less than one.

In order to illustrate this, let us first consider the case $n = 1$ for which equations (2.6) and (2.9) yield

$$\Pi_1 = \int_0^\infty \mu'(t) e^{-\mu(t)} dt = - \int_0^\infty \frac{d}{dt} e^{-\mu(t)} dt = 1 - e^{-\mu(\infty)}.$$

Thus, $\Pi_1 < 1$ if $\mu(\infty) < \infty$. In order to extend this result for $n > 1$, we rewrite equations (2.6) and (2.9) as

$$\Pi_n = \frac{1}{n!} \int_0^\infty e^{-\mu(t)} \frac{d}{dt} \mu(t)^n dt. \quad (2.11)$$

Integrating by parts yields

$$\Pi_n = \frac{\mu(\infty)^n}{n!} e^{-\mu(\infty)} + \frac{1}{n!} \int_0^\infty \mu'(t) \mu(t)^n e^{-\mu(t)} dt, \quad (2.12)$$

which implies that

$$\Pi_{n+1} = \Pi_n - \frac{\mu(\infty)^n}{n!} e^{-\mu(\infty)}. \quad (2.13)$$

After substituting Π_1 into the recursion relation (2.13) and solving we have that

$$\Pi_n = 1 - \sum_{k=0}^{n-1} \frac{\mu(\infty)^k}{k!} e^{-\mu(\infty)}. \quad (2.14)$$

If $\mu(\infty) < \infty$ is finite then $1 > \Pi_1 > \Pi_2 > \dots > \Pi_n$ and $\Pi_n \rightarrow 0$ in the limit $n \rightarrow \infty$. On the other hand, if $\mu(t) \rightarrow \infty$ as $t \rightarrow \infty$, we have $\Pi_n = 1$ for all $n \geq 1$. Note that one can also derive (2.14) with $\Pi_n = \lim_{t \rightarrow \infty} F_n(t)$ using (2.8).

Mean-field limit

One major assumption of our population model is that there is a sufficient number of particles N within the search domain so that we can neglect the flux of particles from the track to the target in equation (2.1). This decoupling of the transport process given by equation (2.1) from the Poisson filling process is essentially a mean-field limit $N \rightarrow \infty$, and leads to a considerable simplification of the analysis. In order to understand this mean-field limit, let us compare the above model with previous stochastic models of a single random intermittent searcher looking for a hidden target at a fixed but unknown location $x = X$, for which $N = 1$ and $n = 1$ [16–21, 24]. In these latter models $u_j(x, t)$ is replaced by the probability density $p_j(x, t)$ of finding the single searcher in state $j = 0, \pm$ at time t and location x , and equation (2.1) becomes

$$\partial_t p_+ = -v \partial_x p_+ - \beta_+ p_+ + \alpha p_0 \quad (2.15a)$$

$$\partial_t p_- = v \partial_x p_- - \beta_- p_- + \alpha p_0 \quad (2.15b)$$

$$\partial_t p_0 = \beta_+ p_+ + \beta_- p_- - 2\alpha p_0 - k \chi([x - X]/l) p_0 \quad (2.15c)$$

with

$$\chi(x) = \begin{cases} 1, & \text{if } |x| < 1 \\ 0, & \text{otherwise.} \end{cases} \quad (2.16)$$

In the case of a single searcher, it is no longer possible to neglect the flux into the target. The target is now treated

as a partially absorbing trap, in which the searcher can detect the target (be absorbed by the trap) at a rate k provided that it is in the stationary state and within a distance l of the target. As in the mean-field model, there are two important quantities characterizing the efficacy of the random intermittent search process [16]. The first is the hitting probability $\Pi^{(1)}$ that a particle starting at $x = 0$ at time $t = 0$ finds the target, that is, the particle is absorbed somewhere within the domain $X - l \leq x \leq X + l$. (The superscript (1) indicates that we are considering a single searcher). The second is the conditional mean first passage time (MFPT) $T^{(1)}$ for the particle to find the target given that it is eventually absorbed by the target. If $J^{(1)}(t)$ denotes the probability flux due to absorption by the target at X

$$J^{(1)}(t) = k \int_{X-l}^{X+l} p_0(x, t) dx. \quad (2.17)$$

then

$$\Pi^{(1)} = \int_0^\infty J^{(1)}(t) dt, \quad T^{(1)} = \frac{\int_0^\infty t J^{(1)}(t) dt}{\int_0^\infty J^{(1)}(t) dt}. \quad (2.18)$$

In order to relate the single searcher model to the mean-field model when the capacity of the trap is $n = 1$, let us consider N independent, identical searchers that all start at the origin at time $t = 0$. Denote the MFPT to find the target of the j th searcher by T_j , $j = 1, \dots, N$, with each T_j and independent, identically distributed random variable drawn from the single searcher first passage time distribution $F^{(1)}(t) = \int_0^t J^{(1)}(s) ds$. The random time T to fill the trap is then given by $T = \min(T_1, T_2, \dots, T_N)$, and the distribution for T is

$$\begin{aligned} F^{(N)}(t) &= \text{Prob}(T < t) = 1 - \text{Prob}(T > t) \\ &= 1 - \text{Prob}(M_1 > t, M_2 > t, \dots, M_N > t) \\ &= 1 - (1 - F^{(1)}(t))^N. \end{aligned}$$

Now suppose that the rate of detection for a single searcher scales as $k = \kappa/N$. This immediately implies that in the large N limit the flux term in equation (2.15c) vanishes, as assumed in the mean-field model. Substituting for $J^{(1)}(s)$ using equation (2.17) then gives

$$F^{(N)}(t) = 1 - \left(1 - \frac{\kappa}{N} \int_0^t \int_{X-l}^{X+l} p_0(x, s) ds \right)^N. \quad (2.19)$$

Finally, taking the large N limit shows that

$$\lim_{N \rightarrow \infty} F^{(N)}(t) = 1 - e^{-\mu(t)} = F_1(t), \quad (2.20)$$

where $F_1(t)$ is the cumulative waiting time distribution (2.8) of the mean-field model for $n = 1$, having identified $p_0(x, t)$ with $u_0(x, t)$. In section IV we will use Monte Carlo simulations for finite N to show that the mean-field approximation of the first passage time density is

quite accurate when $N = \mathcal{O}(100)$, at least in the case of biased searches.

Note that the relationship between the first passage time density of a single searcher and a set of N independent searchers has recently been studied in some detail by Mejia-Monasterio *et al.* Ref. [33]. Assuming a general parametric form for the single searcher first passage time density, they analyze the distribution $P(\omega)$ of the random variable $\omega = T_1 / \sum_{j=1}^N T_j$, and show that in certain situations the MFPT is not a robust measure of search efficiency.

III. CALCULATION OF $\mu(t)$

So far we have shown how the waiting time density $f_n(t)$ for filling a Poisson trap depends on the integrated probability flux

$$\mu(t) = \kappa \int_0^t \int_{X-l}^{X+l} u_0(x, s) dx ds, \quad (3.1)$$

with $p_0(x, s)$ obtained by solving the linear reaction-hyperbolic equations (2.1) under the specified initial and boundary conditions. In the case of the 3-state model of random intermittent search, it is possible to solve the full model using Laplace transform methods for example [16, 18]. However, such an approach becomes considerably more difficult when the complexity of the molecular motor model increases [34, 35] or the search domain becomes more complex eg. branching dendrites and axons [17] and higher-dimensional search processes [19, 20, 36]. However, as we have shown elsewhere for single searcher models [17, 24], it is possible to carry out a quasi-steady state (QSS) reduction of the linear reaction-hyperbolic equations, which yields a one-dimensional advection-diffusion equation (or a corresponding Fokker-Planck equation in the case of the probabilistic version (2.15)). This reduction is based on the observation that the state transition rates of the molecular motor complex are fast compared to the characteristic velocities. A number of authors have analyzed linear reaction-hyperbolic equations in this regime but have focused on the wave-like properties of the transport process rather than the delivery of cargo to hidden targets [14, 28–30]. In this section we carry out the QSS reduction of the population model, and then use this to determine $\mu(t)$. Since, the reduction is very similar to the single searcher case, we only sketch the basic steps of the QSS reduction. Further details can be found in previous papers [17, 24].

Quasi-steady state approximation

First, it is necessary to non-dimensionalize equation (2.1) by rescaling space and time according to

$$x \rightarrow x/\Delta, \quad t \rightarrow tv/\Delta,$$

where Δ is a fundamental length scale of the system. In the case of a finite track of length L , we could set $\Delta = L$ as in Ref. [14]. On the other hand, for a semi-infinite track with a single target, we can identify Δ either with the size of the target l or the distance X of the target from the origin. Since l may be taken to be arbitrarily small (by an appropriate rescaling of the rate κ), we set $\Delta = X$. Assuming that the transition rates α, β_{\pm} are large compared to v/Δ , we introduce the dimensionless parameters $a = \epsilon\alpha\Delta/v$ and $b_{\pm} = \epsilon\beta_{\pm}\Delta/v$ where $\epsilon \ll 1$. The transport equations (2.1) then become

$$\partial_t u_+ = \frac{1}{\epsilon}(-b_+ u_+ + a u_0) - \partial_x u_+ \quad (3.2a)$$

$$\partial_t u_- = \frac{1}{\epsilon}(-b_- u_- + a u_0) + \partial_x u_- \quad (3.2b)$$

$$\partial_t u_0 = \frac{1}{\epsilon}(b_+ u_+ + b_- u_- - 2a u_0) \quad (3.2c)$$

which can be rewritten in the matrix form

$$\partial_t \mathbf{u} = \frac{1}{\epsilon} A \mathbf{u} + \mathcal{L}(\mathbf{u}), \quad (3.3)$$

where $\mathbf{u} = (u_+, u_-, u_0)^{\text{tr}}$, A is the matrix

$$A = \begin{bmatrix} -b_+ & 0 & a \\ 0 & -b_- & a \\ b_+ & b_- & -2a \end{bmatrix}, \quad (3.4)$$

and \mathcal{L} is the linear operator

$$\mathcal{L}(\mathbf{u}) = \begin{bmatrix} -\partial_x u_+ \\ \partial_x u_- \\ 0 \end{bmatrix}. \quad (3.5)$$

The left nullspace of the matrix A is spanned by the vector $\mathbf{e}_L = (1, 1, 1)^{\text{tr}}$ and the right nullspace is spanned by $\mathbf{u}^{ss} = \gamma^{-1}(1/b_+, 1/b_-, 1/a)^{\text{tr}}$. The normalization factor γ is chosen so that $\mathbf{e}_L \cdot \mathbf{u}^{ss} = 1$, that is, $\gamma = b_+^{-1} + b_-^{-1} + a^{-1}$. Let $\phi = \mathbf{e}_L \cdot \mathbf{u}$ and $\mathbf{w} = \mathbf{u} - \phi \mathbf{u}^{ss}$ such that $\mathbf{e}_L \cdot \mathbf{w} = 0$. We can interpret ϕ as the component of \mathbf{u} in the left nullspace of A , whereas \mathbf{w} is in the orthogonal complement.

Multiplying both sides of (3.3) by \mathbf{e}_L^{tr} we obtain

$$\partial_t \phi = \mathbf{e}_L^{\text{tr}} \mathcal{L}(\phi \mathbf{u}^{ss} + \mathbf{w}). \quad (3.6)$$

Substituting $\mathbf{u} = \mathbf{w} + \phi \mathbf{u}^{ss}$ into (3.3) yields

$$\partial_t \mathbf{w} + (\partial_t \phi) \mathbf{u}^{ss} = \frac{1}{\epsilon} A (\mathbf{w} + \phi \mathbf{u}^{ss}) + \mathcal{L}(\mathbf{w} + \phi \mathbf{u}^{ss}). \quad (3.7)$$

Using equation (3.6) and the fact that \mathbf{u}^{ss} is in the right null space of A , we obtain

$$\partial_t \mathbf{w} = \frac{1}{\epsilon} A \mathbf{w} + (\mathbb{I}_3 - \mathbf{u}^{ss} \mathbf{e}_L^{\text{tr}}) \mathcal{L}(\mathbf{w} + \phi \mathbf{u}^{ss}), \quad (3.8)$$

where \mathbb{I}_3 is the 3×3 identity matrix. Now introduce an asymptotic expansion for \mathbf{w} of the form

$$\mathbf{w} \sim \mathbf{w}_0 + \epsilon \mathbf{w}_1 + \epsilon^2 \mathbf{w}_2 + \dots \quad (3.9)$$

After substituting this expansion into (3.8) and collecting $\mathcal{O}(\epsilon^{-1})$ terms we see that $A\mathbf{w}_0 = 0$. Since \mathbf{w} is in the orthogonal complement of the left nullspace of A , it follows that $\mathbf{w}_0 = 0$. Now collecting terms of $\mathcal{O}(1)$ yields the equation

$$A\mathbf{w}_1 = -(\mathbb{I}_3 - \mathbf{u}^{ss}\mathbf{e}_L^{\text{tr}})\mathcal{L}(\phi\mathbf{u}^{ss}). \quad (3.10)$$

Although the matrix A is singular, the orthogonal projection operator $(\mathbb{I}_3 - \mathbf{u}^{ss}\mathbf{e}_L^{\text{tr}})$ ensures that the right-hand side of the above equation is in the range of A . By the Fredholm alternative theorem a solution \mathbf{w}_1 exists, and is unique after imposing the normalization condition $\mathbf{e}_L \cdot \mathbf{w} = 0$. Finally, substituting the resulting solution for \mathbf{w}_1 back into (3.6) yields the advection-diffusion equation [24]

$$\frac{\partial \phi}{\partial t} = -V \frac{\partial \phi}{\partial x} + D \frac{\partial^2 \phi}{\partial x^2} \quad (3.11)$$

where

$$V = \frac{1}{\gamma} \left(\frac{1}{b_+} - \frac{1}{b_-} \right) \quad (3.12)$$

$$D = \epsilon \left(\frac{(1 - V_0)^2}{\gamma b_+^2} + \frac{(1 + V_0)^2}{\gamma b_-^2} \right). \quad (3.13)$$

The function ϕ is the total concentration of all particles at position x and time t .

Equation (3.11) is supplemented by a Neumann boundary condition at $x = 0$ of the form

$$-V\phi(0, t) + D \left. \frac{\partial \phi}{\partial x} \right|_{x=0} = 0. \quad (3.14)$$

This boundary condition follows from substituting $\mathbf{u} = \phi\mathbf{u}^{ss} + \epsilon\mathbf{w}_1$ into the boundary condition (2.2) of the corresponding 3-state model (2.1). The associated initial condition is $\phi(x, 0) = U\delta(x)$. The solution of equation (3.11) is then a classical result based on the method of images [37]:

$$\phi(x, t) = \frac{1}{\sqrt{\pi Dt}} e^{-[x - Vt]^2/(4Dt)} - \frac{V}{2D} e^{xV/D} \text{erfc} \left(\frac{x + Vt}{2\sqrt{Dt}} \right). \quad (3.15)$$

Note that although we have carried out the QSS reduction for the specific 3-state model, the same procedure can be applied to more complex molecular motor models. One still obtains the advection-diffusion equation (3.11) and associated solution (3.15) [24]. The only difference is the explicit dependence of the drift and diffusion parameters V, D on model parameters.

Asymptotics

Given the solution (3.15) for $\phi(x, t)$, the rate $\lambda(t)$ of the Poisson filling process is determined according to

$$\lambda(t) = \hat{\kappa} \int_{X-l}^{X+l} \phi(x, t) dx, \quad (3.16)$$

where $\hat{\kappa} = \kappa/(a\gamma)$. For simplicity, we assume that $l \ll X$ and take $\lambda(t) = 2l\hat{\kappa}\phi(X, t)$. Under this approximation

$$\mu(t) = c \int_0^t \phi(X, t) dt. \quad (3.17)$$

For convenience, we have set $2l\hat{\kappa} = c$. Unfortunately, it is not possible to derive an explicit analytical solution for $\mu(t)$, although the integral expressions can be evaluated numerically. Nevertheless, we can obtain the exact hitting probability Π_M , and we can asymptotically determine the large-time behavior of the waiting time density.

First, recall from equation (2.14) that the hitting probability Π_n is determined by $\mu(\infty)$. The latter can be calculated using Fourier-Laplace transforms. We begin by rewriting the right-hand side of equation (3.15) in terms of Fourier transforms. That is, set $\phi(x, t) = 2\phi_0(x, t) - (V/2D)e^{xV/D}\phi_1(x, t)$ with

$$\begin{aligned} \phi_0(x, t) &\equiv \frac{1}{\sqrt{4\pi Dt}} e^{-[x - Vt]^2/(4Dt)} \\ &= \int_{-\infty}^{\infty} e^{ik[x - Vt]} e^{-Dtk^2} \frac{dk}{2\pi} \end{aligned} \quad (3.18)$$

and

$$\begin{aligned} \phi_1(x, t) &\equiv \text{erfc} \left(\frac{x + Vt}{2\sqrt{Dt}} \right) \\ &= \frac{2}{\sqrt{\pi}} \int_{(x+Vt)/\sqrt{4Dt}}^{\infty} e^{-u^2} du \\ &= 2 \int_0^{\infty} \int_{-\infty}^{\infty} e^{ik[y+x+Vt]} e^{-Dtk^2} \frac{dk}{2\pi} dy. \end{aligned} \quad (3.19)$$

Now consider the Laplace transform

$$\tilde{\phi}(x, s) = \int_0^{\infty} e^{-st} \phi(x, t) dt. \quad (3.20)$$

Substituting for ϕ_0 and ϕ_1 and integrating with respect to t then gives

$$\begin{aligned} \tilde{\phi}(x, s) &= 2 \int_{-\infty}^{\infty} \frac{e^{ikx}}{ikV + Dk^2 + s} \frac{dk}{2\pi} \\ &\quad - \frac{V}{D} e^{xV/D} \int_0^{\infty} \int_{-\infty}^{\infty} \frac{e^{ik(x+y)}}{(Dk^2 - ikV + s)} \frac{dk}{2\pi} dy. \end{aligned} \quad (3.21)$$

The integrals with respect to k can be evaluated by closing the contour in the upper-half complex plane:

$$\begin{aligned} \tilde{\phi}(x, s) &= 2 \frac{e^{-[\Gamma(s) - V/2D]x}}{\sqrt{V^2 + 4sD}} \\ &\quad - \frac{V}{D} e^{xV/D} \int_0^{\infty} \frac{e^{-[\Gamma(s) + V/2D](x+y)}}{\sqrt{V^2 + 4sD}} dy, \\ &= \frac{e^{-[\Gamma(s) - V/2D]x}}{\sqrt{V^2 + 4sD}} \left[2 - \frac{V}{D} \frac{1}{\Gamma(s) + V/2D} \right] \end{aligned} \quad (3.22)$$

with

$$\Gamma(s) = \frac{1}{2} \sqrt{(V/D)^2 + 4s/D}. \quad (3.23)$$

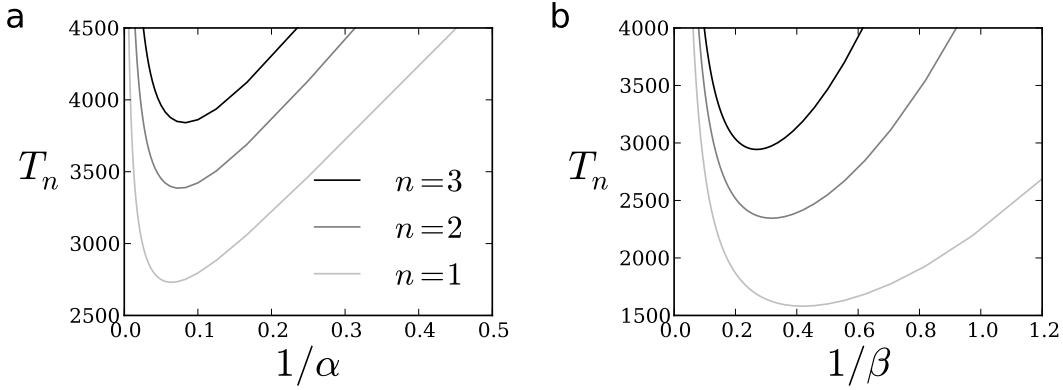


FIG. 2. Unbiased ($\beta_+ = \beta_- = \beta$) random intermittent search in the mean-field population model. The MFPT vs the (a) average search time and (b) the average duration of the moving (forward and backward) state for different values of the Poisson trap size n . Each curve has a minimum MFPT for a given value of α and β . Parameter values used are $\epsilon = 0.1$, $k = 5/N$, $X = 50$, and $l = 0.25$. For (a) we use $\beta = 1/\epsilon$ and for (b) we use $\alpha = 2/\epsilon$.

It follows from equation (3.17) that

$$\mu(\infty) = c \lim_{s \rightarrow 0} \tilde{\phi}(X, s) = \frac{c}{V}. \quad (3.24)$$

Thus the corresponding hitting probability $\Pi_n < 1$ for $V > 0$ and $\Pi_n = 1$ for $V = 0$ (pure diffusion).

We now estimate the large- t behavior of $\phi(X, t)$ in order to approximate $\mu(t)$. We use the following asymptotic expansion of the complementary error function:

$$\text{erfc}(z) = \frac{e^{-z^2}}{\sqrt{\pi}z} \left[1 - \frac{1}{2z^2} \dots \right]. \quad (3.25)$$

Applying this to equation (3.15) with $z = (x + Vt)/(2\sqrt{Dt}) \approx V\sqrt{t}/(2\sqrt{D})$ for large t and $V > 0$, we obtain the approximation

$$\phi(X, t) \sim \frac{2c\sqrt{D}}{V^2\sqrt{\pi t^3}} e^{-V^2 t/(4D)}, \quad (3.26)$$

which is independent of target location X . Substituting this expression into equation (3.17) gives

$$\begin{aligned} \mu(t) &\sim \mu(\infty) - \frac{2c\sqrt{D}}{V^2\sqrt{\pi}} \int_t^\infty \frac{1}{\sqrt{t'^3}} e^{-V^2 t'/(4D)} dt' \\ &= \mu(\infty) - \frac{2c}{V\sqrt{\pi}} \int_{\sqrt{tV^2/4D}}^\infty u^{-2} e^{-u^2} du \\ &\sim \mu(\infty) - \frac{2c}{V\sqrt{\pi}} \left[\frac{4D}{tV^2} \right]^{3/2} e^{-V^2 t/(4D)}, \end{aligned} \quad (3.27)$$

using an asymptotic expansion of the integral. On the other hand, for $V = 0$, we have

$$\begin{aligned} \mu(t) &= c \int_0^t \frac{1}{\sqrt{\pi Dt}} e^{-X^2/(4Dt)} \\ &\sim 2c\sqrt{t/\pi D}, \end{aligned} \quad (3.28)$$

where we have used the approximation $e^{-X^2/(4Dt)} \sim 1$ for large t .

The large-time asymptotic approximation for $\mu(t)$ determines how the waiting time density, $f_n(t)$, scales with time. Equations (2.9) and (3.27) imply that for $V = 0$:

$$f_n(t) \propto t^{n/2-1} e^{-\hat{c}\sqrt{t}}, \quad (3.29)$$

with $\hat{c} = 2c/\sqrt{\pi D}$. Extensions to the case $V > 0$ are a little more involved. However, for $n = 1$ we have

$$f_1(t) \propto t^{-1/2} e^{-V^2 t/(4D)}. \quad (3.30)$$

IV. RESULTS

In the case of a single random intermittent searcher on a finite track of length L with reflecting boundary conditions at both ends $x = 0, L$ (so that $\Pi^{(1)} = 1$) and unbiased transport ($\beta_+ = \beta_- = \beta$), it can be shown that there exists an optimal search strategy in the sense that there exists a unique set of transition rates α, β for which the MFPT is minimized [18–21]. On the other hand, for directed intermittent search ($\beta_+ > \beta_-$) on a semi-infinite domain or a finite domain with an absorbing boundary at $x = L$ (so that $\Pi^{(1)} < 1$), a unique optimal strategy no longer exists [16, 24]. In this section, we show that a similar situation holds if there is a population of N independent searchers and we consider the time necessary for $n < N$ of those searchers to locate the target. Note that the previous results for the single-searcher process are recovered by setting $n = N = 1$. For the case where $n \ll N$, we use the mean-field approximation, and for smaller values of N , we use Monte-Carlo simulations with the target detection rate, k , scaled by the number of searchers (i.e. $k \rightarrow k/N$).

First, we consider an unbiased random intermittent search process in the mean-field population model, for

which $N \rightarrow \infty$ and $\beta_+ = \beta_- = \beta$ ($V = 0$). In Fig. 2 the MFPT is plotted as a function of (a) the average duration of the search phase, $1/\alpha$, and (b) the average duration of the ballistic phase, $1/\beta$. For each value of trap capacity $n = 1, 2, 3$, we see that there exists a minimum MFPT for a particular choice of α, β , consistent with the single-searcher regime. Next, we examine how the search process changes as more searchers are added for fixed $n = 1$. In particular, the first passage time density is approximated by Monte-Carlo simulations for different values of N , and the results are compared to the analytical mean field results. This gives a nice illustration of how the single-searcher process ($N = 1$) is related to the mean-field population search process ($N \rightarrow \infty$). In Fig. 3, the unbiased case is shown. The most significant

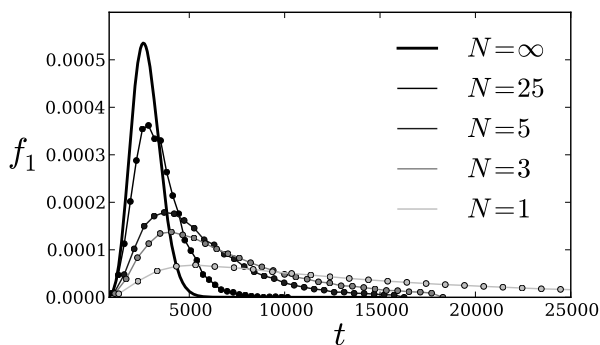


FIG. 3. First passage time density for an unbiased search and a single-capacity trap ($n = 1$). The solid curve shows the analytical density function in the mean field limit and the remaining curves are histograms obtained from 10^4 Monte-Carlo simulations for different numbers of searchers N . Parameter values are the same as in Fig. 2.

difference is found in the large time behavior, with power-law scaling $t^{-3/2}$ for the single search and the so-called stretched exponential scaling $e^{-\hat{c}\sqrt{t}}$ (see Eqn. (3.29)) for the mean field $N \rightarrow \infty$ limit. A similar plot showing the first passage time density for a biased search ($\beta_+ < \beta_-$ so that $V > 0$) is shown in Fig. 4. In this case, adding more searchers has little qualitative effect on the first passage time density, each case having the same exponential large time scaling (see Eqn. (3.29)). In both cases, the results, show that adding more searchers decreases the mean search time and the variance.

Our analysis of the mean-field model showed that the hitting probability is less than unity when the velocity bias is positive (i.e. when $\beta_+ < \beta_-$ so that $V > 0$). Therefore, we would like to quantify how the hitting probability and the MFPT change as we vary the amount of bias. In Fig. 5, we plot the MFPT vs. the hitting probability for different values of N . Each curve is parameterized by β_+ , the rate of leaving the forward-moving state, with $0 < \beta_+ < \beta_-$. By changing the value of β_+ , any hitting probability can be achieved. As $\beta_+ \rightarrow \beta_-$ the searcher's motion becomes unbiased, and the hitting

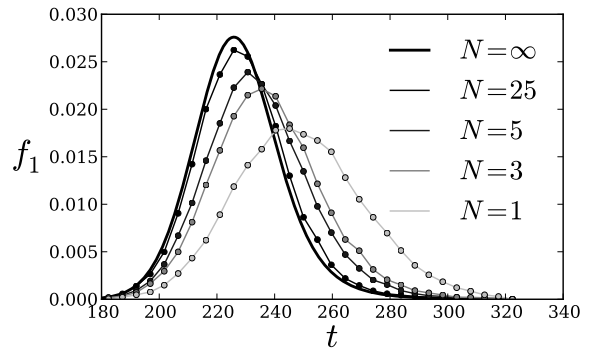


FIG. 4. First passage time density for a biased search and a single-capacity trap ($n = 1$). The black curve shows the analytical density function in the mean-field limit, and the remaining curves are histograms obtained from 5×10^4 Monte-Carlo simulations. Parameter values used are $\alpha = 1/\epsilon$, $\beta_+ = 1/\epsilon$, $\beta_- = 2/\epsilon$, $\epsilon = 0.1$, $k = 5/N$, $X = 50$, and $l = 0.25$.

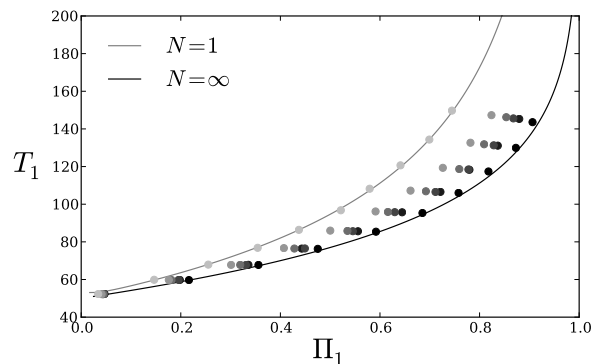


FIG. 5. The MFPT vs hitting probability for the single capacity trap ($n = 1$). Each curve is parameterized by $0 \leq \beta_+ \leq \beta_-$. Analytical results are shown as lines, with the single searcher in grey and the mean field limit ($N = \infty$) in black. Averaged Monte Carlo simulations (10^4 simulation each) are shown as symbols, sets ranging from grey to black, with a different value of N used in each set. From grey to black there are six sets of simulations with $N = 1, 2, 3, 4, 5, 25$, respectively. Parameter values are the same as in Fig. 4.

probability increases to unity. However, as the searchers become more unbiased the MFPT also increases. Analytical results for the single searcher case ($N = 1$) and the mean-field limit ($N = \infty$) are shown as solid curves (black and grey, respectively) and to connect the two, averaged Monte-Carlo simulations are shown (as dots) for different values of $N = 1, 2, 3, 4, 25$ (each dot is colored in greyscale from $N = 1$ in black to $N = 25$ in light grey). Ten different sets of Monte-Carlo simulations are run corresponding to ten different values of β_+ , and in each set the hitting probability decreases and the MFPT increases as more searchers are added.

We now turn our attention to how increasing the trap capacity affects the search process in the mean-field

limit; that is, we examine how the first passage time density, MFPT, and hitting probability change as we increase n . First, we plot the first passage time density, for (a) $V = 0$ and (b) $V > 0$, in Fig. 6. In both cases,

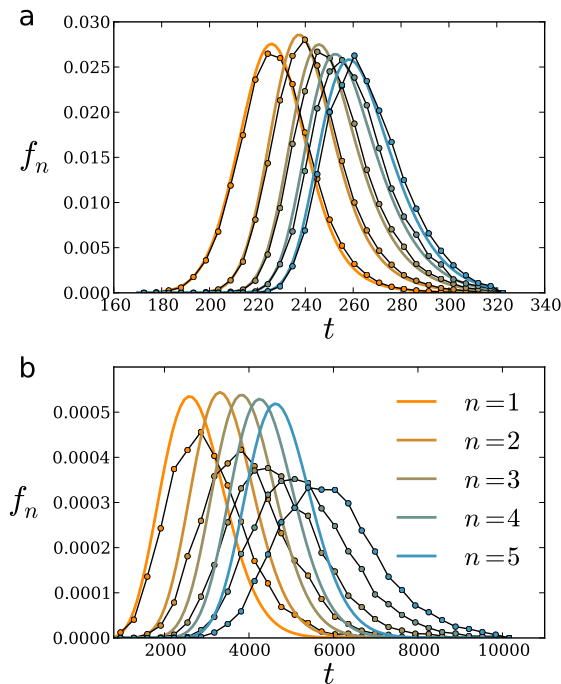


FIG. 6. The first passage time density for different values of n . Solid curves show the mean field limit and histograms are generated from 10^4 Monte-Carlo simulations with $N = 50$ searchers. (a) The unbiased case $V = 0$. (b) The biased case $V > 0$. Parameter values used are the same as in Fig. 2 and Fig. 4 for (a) and (b), respectively.

increasing the trap capacity increases the MFPT. It is worth commenting that when the searchers are unbiased, there is less quantitative agreement between the mean field limit and histograms generated by Monte-Carlo simulations with $N = 50$ searchers. Finally, as we did in Fig. 5, the MFPT and hitting probability are shown for the biased search in Fig. 7, this time for different trap capacities. As expected, the hitting probability decreases and the MFPT increases as we increase the capacity of the trap.

V. DISCUSSION

In this paper, we have extended the theory of random intermittent search to a population model of N independent searchers looking to deliver cargo to a single hidden target. We have analyzed the model in the mean-field limit $N \rightarrow \infty$, where the concentrations of particles evolve according to a system of linear reaction-hyperbolic equations that decouples from the Poisson process associated with filling the target with cargo. We compared

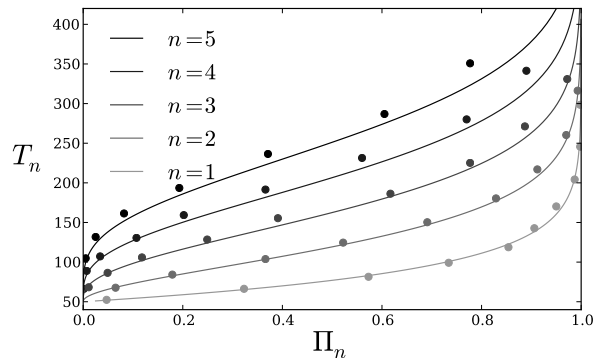


FIG. 7. The MFPT vs hitting probability for different trap capacities n . Each curve is parameterized by $0 \leq \beta_+ \leq \beta_-$. The mean-field limit is shown as solid curves, and 10^3 averaged Monte-Carlo simulations with $N = 50$ are shown as symbols. Parameter values are the same as in Fig. 4.

our analytical results with Monte-Carlo simulations for finite N and thus determined how the efficiency of the search process depends on N and the capacity n of the target.

There are a number of possible extensions of our work. First, within the context of dendritic and axonal transport, we could consider more detailed biophysical models of single motor-cargo complexes, which take into account possible local signaling mechanisms between the target and searcher. Indeed, elsewhere we have applied the QSS reduction to a multiple motor model of bidirectional transport, in which opposing motors compete in a “tug-of-war” [38], and showed how the concentration of adenosine triphosphate (ATP) or signaling molecules such as microtubule associated proteins (MAPs) could regulate the delivery of cargo to synaptic targets [17, 34, 35]. These details could be incorporated into our mean-field population model under the QSS reduction, since it would simply involve determining the dependence of the effective diffusivity D and drift V on the relevant biophysical parameters. Combined with Monte-Carlo simulations, we could then investigate the efficiency of the cargo delivery process as a function of N and n , along similar lines to the current paper. Incorporating local signaling mechanisms from synaptic targets would allow us to explore the role of motor transport in synaptic plasticity [15], for example.

Another possible generalization would be to consider multiple searchers looking for multiple hidden targets. In this case, targets could compete with one another for resources. Moreover, there would be effective statistical correlations due to the fact that one would need to keep track of which targets have been filled and at what times, since filled targets would no longer act as traps for searching particles. Yet another extension would be to introduce interactions between the searching particles. In the case of molecular motor transport, this could arise due to molecular crowding resulting in exclusion effects.

In other types of search such as foraging, there could be communication between searchers.

ACKNOWLEDGEMENTS

This publication was based on work supported in part by the National Science Foundation (DMS-1120327) and by Award No KUK-C1-013-4 made by King Abdullah University of Science and Technology (KAUST).

APPENDIX

In this appendix we show how the Poisson process for filling the trap can be approximated by a Gaussian process in the large M limit, where M is the capacity of the trap. Such an approximation also serves as an illustrative model of a trap that is filled continuously rather than in discrete jumps. First, note that the probability distribution $P(n, t)$ satisfies the master equation

$$\frac{\partial P(n, t)}{\partial t} = \lambda(t)P(n-1, t) - \lambda(t)P(n, t). \quad (\text{A.1})$$

Performing the change of variables $q = n/M$ such that $P(n, t) \rightarrow P(q, t)$ and $P(n-1, t) \rightarrow P(q - \epsilon, t)$ with $\epsilon = 1/N$, we can Taylor expand the master equation to second order in ϵ to obtain the Gaussian approximation [39]

$$\frac{\partial P(q, t)}{\partial t} = -\epsilon\lambda(t)\frac{\partial P}{\partial q} + \frac{\epsilon^2\lambda(t)}{2}\frac{\partial^2 P}{\partial q^2}. \quad (\text{A.2})$$

The resulting Fokker-Planck equation determines the probability density of a corresponding stochastic process $Q(t)$ evolving according to the Langevin equation

$$dQ = \epsilon\lambda(t) + \epsilon\sqrt{\lambda(t)}dW(t) \quad (\text{A.3})$$

where $W(t)$ is a Wiener process. Under the Gaussian approximation, calculation of the waiting time density $f_M(t)$ translates into calculation of the first passage time density $f_Q(t)$ for reaching $Q(t) = 1$ given that $Q(0) = 0$. As a further simplification, we allow $Q(t)$ to take on negative values by taking $-\infty < Q \leq 1$ with an absorbing boundary at $Q = 1$, that is, $P(1, t) = 0$. (Physically speaking $0 \leq Q \leq 1$, but the probability of the Langevin process crossing into the negative half-line is relatively small). Given the solution of the Fokker-Planck equation (A.2), we define the survival function $F_Q(t) = \int_{-\infty}^1 P(q, t)dq$ which then determines the first passage time density according to

$$f_Q(t) = -\frac{dF_Q}{dt} = -\frac{\epsilon^2\lambda(t)}{2}\frac{\partial P(q, t)}{\partial q}\bigg|_{q=1}. \quad (\text{A.4})$$

Since the ratio of the variance over the mean is time-independent, we can adapt the recent analysis of time-dependent Fokker-Planck equations based on the method of images Ref. [37]. The first step is to find the solution $P_0(q, t|q_0)$ of equation (A.2) on \mathbb{R} given the initial condition $P_0(q, 0|q_0) = \delta(q - q_0)$. Under the change of variables

$$\tau = \frac{\epsilon^2}{2} \int_0^t \lambda(s)ds = S(t) \quad (\text{A.5})$$

$$z = q - \epsilon \int_0^t \lambda(s)ds = q - \Sigma(t), \quad (\text{A.6})$$

equation (A.2) becomes [37]

$$\frac{\partial P_0}{\partial \tau} = \frac{\partial^2 P_0}{\partial z^2} \quad (\text{A.7})$$

with $-\infty < z < \infty$. Solving this standard diffusion equation with the given initial condition, we have in original coordinates

$$P_0(q, t|q_0) = \frac{1}{2\sqrt{\pi S(t)}} e^{-[q - q_0 - \Sigma(t)]^2/(4S(t))}. \quad (\text{A.8})$$

Now suppose that there is an absorbing boundary at $q = 1$. Under the method of images we solve equation (A.2) on \mathbb{R} but introduce an image source at some location q_0 with $q_0 > 1$ in order to maintain the boundary condition $p(1, t) = 0$. That is, we take the initial condition to be [37]

$$P(q, 0) = \delta(q) - e^{-\eta}\delta(q - q_0) \quad (\text{A.9})$$

so that

$$P(q, t) = P_0(q, t|0) - e^{-\eta}P_0(q, t|q_0). \quad (\text{A.10})$$

Imposing the boundary condition $P(1, t) = 0$ and using the solution (A.8), we obtain the condition

$$\frac{[1 - \Sigma(t)]^2}{4S(t)} = \frac{[1 - q_0 - \Sigma(t)]^2}{4S(t)} + \eta. \quad (\text{A.11})$$

As $t \rightarrow 0$, $\Sigma(t), S(t) \rightarrow 0$ so that $1 = (1 - q_0)^2$, which implies that $q_0 = 2$. Setting $q_0 = 2$ in equation (A.11) then implies that $\Sigma(t)/S(t) = -\eta$. Thus, the above solution is only valid if the ratio of the variance and the mean of the Langevin process is time-independent. This condition holds for the Gaussian approximation of the Poisson process, with $\Sigma(t) = \epsilon\mu(t)$ and $S(t) = \epsilon^2\mu(t)/2$. Thus, $\eta = -2/\epsilon$. We conclude that

$$P(q, t) = \frac{1}{\sqrt{2\pi\epsilon^2\mu(t)}} \left[e^{-[q - \epsilon\mu(t)]^2/(2\epsilon^2\mu(t))} - e^{2/\epsilon} e^{-[q - 2 - \epsilon\mu(t)]^2/(2\epsilon^2\mu(t))} \right]. \quad (\text{A.12})$$

Finally, equation (A.4) shows that

$$f_Q(t) = \frac{\lambda(t)}{\sqrt{2\pi\epsilon^2\mu(t)^{3/2}}} e^{-[1 - \epsilon\mu(t)]^2/(2\epsilon^2\mu(t))}. \quad (\text{A.13})$$

-
- [1] J. W. Bell, *Searching Behaviour, The Behavioural Ecology of Finding Resources* (London: Chapman and Hall, 1991) .
- [2] G. M. Viswanathan, V. Afanasyev, S. V. Buldyrev, E. J. Murphy, H. A. Prince and H. E. Stanley, *Nature* **381**, 413 (1996).
- [3] G. M. Viswanathan, S. V. Buldyrev, S. Havlin, M. G. E. da Luz, E. P. Raposo and H. E. Stanley, *Nature*, **401**, 911 (1999).
- [4] F. Bartumeus, J. Catalan, U. L. Fulco, M. L. Lyra and G. M. Viswanathan, *Phys. Rev. Lett.*, **88**, 097901 (2002).
- [5] A. Caspi, R. Granek and M. Elbaum, *Phys. Rev. E* **66**, 011916 (2002).
- [6] D. Arcizet, B. Meier, E. Sackmann, J. O. Radler and D. Heinrich, *Phys. Rev. Lett.* **101**, 248103 (2008).
- [7] S. Klumpp and R. Lipowsky, *Phys. Rev. Lett.* **95**, 268102 (2005).
- [8] C. Loverdo, O. Benichou, M. Moreau and R. Voituriez, *Nature Phys.* **4**, 134 (2008).
- [9] A. Kahana, G. Kenan, M. Feingold, M. Elbaum and R. Granek, *Phys. Rev. E* **78**, 051912 (2008).
- [10] O. G. Berg and C. Blomberg, *Biophys. Chem.* **4**, 367 (1976).
- [11] S. E. Halford and J. F. Marko. *Nucleic Acids Res.*, **32** 3040 (2004).
- [12] M. Slutsky and L. A. Mirny, *Biophys. J.*, **87** 1640; 4021 (2004).
- [13] M. Coppey, O. Benichou, R. Voituriez and M. Moreau, *Biophys. J.* **87**, 1640 (2004).
- [14] M. C. Reed, S. Venakides, and J. J. Blum, *SIAM J. Appl. Math.* **50**: 167–180, 1990.
- [15] C. R. Bramham and D. G. Wells, *Nat. Rev. Neurosci.* **8**, 776 (2007).
- [16] P. C. Bressloff and J. Newby, *New J. Phys.* **11**, 023033 (2009).
- [17] J. Newby and P. C. Bressloff *Phys. Rev. E*, **80**, 021913 (2009).
- [18] O. Benichou, M. Coppey, M. Moreau, P. H. Suet and R. Voituriez, *Phys. Rev. Lett.* **19**, 198101 (2005).
- [19] O. Benichou, C. Loverdo, M. Moreau and R. Voituriez, *J. Phys. Cond. Matt.* **19**, 065141 (2007).
- [20] C. Loverdo, O. Benichou, M. Moreau and R. Voituriez, *Phys. Rev. E* **80**, 031146 (2009).
- [21] O. Bénichou, C. Loverdo, M. Moreau, and R. Voituriez. Intermittent search strategies. *Rev. Mod. Phys.*, **83** 81 (2011).
- [22] Rook M S, Lu M and Kosik K S J. *Neurosci.* **20** 6385–6393 (2000)
- [23] J. L. Dynes and O. Steward, *J. Comp. Neurol.* **500**, 433 (2007).
- [24] J. Newby and P. C. Bressloff, *Bull. Math. Biol.* **72**, 1840 (2010).
- [25] G. Oshanin, H. Wio, K. Lindenberg, and S. Burlatsky. *Journal of Physics: Condensed Matter*, 19(6):065142, 2007.
- [26] Gleb Oshanin, Katja Lindenberg, Horacio Wio, and Sergei Burlatsky. *J. Phys. A* 42(43):434008, 2009.
- [27] F. Rojo, C. E. Budde, and H. S. Wio. *J. Phys. A* 42(12):125002, 2009.
- [28] A. Friedman and G. Craciun, *SIAM J. Math. Anal.*, 38:741–758, 2006.
- [29] A. Friedman and B. Hu, *Indiana Univ. Math. J.*, 56:2133–2158, 2007.
- [30] E. Brooks, *Ann. Appl. Prob.*, 9:719–731, 1999.
- [31] L. Popovic, S. A. McKinley and M. C. Reed. *SIAM J. Appl. Math.* **71** 1531–1556 (2011).
- [32] H. M. Taylor and S. Karlin *An introduction to stochastic modeling 3rd ed.* Academic Press, San Diego (1998).
- [33] C. Mejia-Monasterio, G. Oshanin and G. Schehr. *J. Stat. Mech.* P06022 (2011).
- [34] J. Newby and P. C. Bressloff, *J. Stat. Mech.* **P04014**, (2010).
- [35] J. Newby and P. C. Bressloff, *Phys. Biol.* **7**, 036004 (2010).
- [36] P. C. Bressloff and J. Newby. *Phys. Rev. E* **83** 061139 (2011).
- [37] A. Molini, P. Talkner, G. G. Katul and A. Porporato. *Physica A* **390** 1841 (2011).
- [38] M. J. I. Mueller, S. Klumpp, and R. Lipowsky *Proc. Nat. Acad. Sci. USA* **105** 4609 (2008).
- [39] C. W. Gardiner. *Handbook of stochastic methods for physics, chemistry, and the natural sciences*, Springer-Verlag, Berlin (1983).

RECENT REPORTS

50/11	Wound healing angiogenesis: the clinical implications of a simple mathematical model	Flegg Byrne Flegg McElwain
51/11	Wound healing angiogenesis: the clinical implications of a simple mathematical model	Du Gunzburger Lehoucq Zhou
52/11	Image Inpainting based on coherence transport with Adapted distance functions	März
53/11	Surface growth kinematics via local curve evolution	Moulton Goriely
54/11	A multiple scales approach to evaporation induced Marangoni convection	Hennessey Münch
55/11	The dynamics of bistable liquid crystal wells	Luo Majumdar Erban
56/11	Real-Time Fluid Effects on Surfaces using the Closest Point Method	Auer Macdonald Treib Schneider Westermann
57/11	Isolating intrinsic noise sources in a stochastic genetic switch	Newby
58/11	Riemann-Cartan Geometry of Nonlinear Dislocation Mechanics	Yavari Goriely
59/11	Helices through 3 or 4 points?	Goriely Neukirch Hausrath
60/11	Bayesian data assimilation in shape registration	Cotter Cotter Vialard
61/11	Asymptotic solution of a model for bilayer organic diodes and solar cells	Richardson Please Kirkpatrick
62/11	Neural field model of binocular rivalry waves	Bressloff Webber
63/11	Front propagation in stochastic neural fields	Bressloff Webber
64/11	Stability estimates for a twisted rod under terminal loads: a three-dimensional study	Majumdar Prior Goriely
65/11	Adaptive Finite Element Method Assisted by Stochastic Simulation of Chemical Systems	Cotter Vejchodsky Erban

66/11	On the shape of force-free field lines in the solar corona	Prior Berger
67/11	Tear film thickness variations and the role of the tear meniscus	Please Fulford Fulford Collins
68/11	Comment on “Frequency-dependent dispersion in porous media”	Davit Quintard
69/11	Molecular Tilt on Monolayer-Protected Nanoparticles	Giomi Bowick Ma Majumdar
70/11	The Capillary Interaction Between Two Vertical Cylinders	Cooray Cicuta Vella
71/11	Nonuniqueness in a minimal model for cell motility	Gallimore Whiteley Waters King Oliver
72/11	Symmetry of uniaxial global Landau-de Gennes minimizers in the theory of nematic liquid crystals	Henao Majumdar

Copies of these, and any other OCCAM reports can be obtained from:

**Oxford Centre for Collaborative Applied Mathematics
Mathematical Institute
24 - 29 St Giles'
Oxford
OX1 3LB
England
www.maths.ox.ac.uk/occam**